



HAL
open science

One-step compatibilization of poly(lactic acid) and tannin via reactive extrusion

Jingjing Liao, Nicolas Brosse, Sandrine Hoppe, Guanben Du, Xiaojian Zhou,
Antonio Pizzi

► **To cite this version:**

Jingjing Liao, Nicolas Brosse, Sandrine Hoppe, Guanben Du, Xiaojian Zhou, et al.. One-step compatibilization of poly(lactic acid) and tannin via reactive extrusion. *Materials & Design*, 2020, pp.108603. 10.1016/j.matdes.2020.108603 . hal-02495239

HAL Id: hal-02495239

<https://hal.science/hal-02495239>

Submitted on 22 Aug 2022

HAL is a multi-disciplinary open access archive for the deposit and dissemination of scientific research documents, whether they are published or not. The documents may come from teaching and research institutions in France or abroad, or from public or private research centers.

L'archive ouverte pluridisciplinaire **HAL**, est destinée au dépôt et à la diffusion de documents scientifiques de niveau recherche, publiés ou non, émanant des établissements d'enseignement et de recherche français ou étrangers, des laboratoires publics ou privés.



Distributed under a Creative Commons Attribution - NonCommercial 4.0 International License

One-step compatibilization of poly (lactic acid) and tannin via reactive extrusion

Jingjing LIAO^{1,2,3}, Nicolas BROSSE^{2*}, Sandrine HOPPE³, Guanben DU^{1*}, Xiaojian ZHOU^{1*}, and Antonio PIZZI²

¹Key Laboratory for Forest Resources Conservation and Utilisation in the Southwest Mountains of China (Southwest Forestry University), Ministry of Education, Kunming, 650224, PR China

²LERMAB, University of Lorraine, Boulevard des Aiguillettes BP 70239, 54506 Vandœuvre-lès-Nancy, France

³LRGP, University of Lorraine, 1, Rue Grandville, BP 451, 54001 Nancy Cedex, France

* Correspondence: nicolas.brosse@univ-lorraine.fr; gongben9@hotmail.com; xiaojianzhou@hotmail.com

Abstract: The compatibility issue between poly(lactic acid) (PLA) and tannin is a big challenge for preparing PLA/tannin biocomposites with enhanced properties. In this work, composites with enhanced properties have been accomplished using an efficient one-step reactive extrusion method with the help of methylene diphenyl diisocyanate (p-MDI) or 3-aminopropytriethoxysilane (APS). The extent of compatibility achieved via the one-step was evaluated by tensile, morphological, rheological, and thermal properties. The obtained results indicated that the adhesion promoters, especially p-MDI, contributed efficiently to an improved tensile behavior of the resulting composites with a tough tensile-fracture surface compared with incompatibilized PLA/tannin composite. Moreover, these composites displayed a plateau-like rheological behavior, enhanced complex viscosity, higher melting and thermal degradation temperature. This approach can be potentially adapted to other PLA/biopolymers composite systems.

Keywords: poly (lactic acid), condensed tannin, reactive extrusion, isocyanate, silane

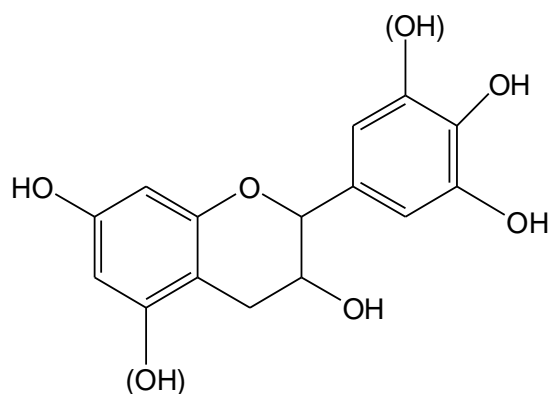
1. Introduction

Poly(lactic acid) (PLA) is a promising green polyester that obtained from agricultural products such as corn, sugar cane, and sugar beet via polycondensation or ring-opening polymerization process [1]. It is one of the most promising candidates to replace fossil-

31 based polymers to develop fully biocomposites as a result of some favorable attributes,
32 such as sustainability, biocompatibility, biodegradability, favorable mechanical
33 properties. PLA is also considered suitable to develop biocomposites with various fibers,
34 fillers and/or polymers [2] through an efficient process like extrusion because of its good
35 thermal processability [3]. Recently, biocomposites consist of PLA and natural fillers are
36 drawing more global attentions since both polymer matrix and fillers are sustainable
37 and degradable, which can minimize the environmental concerns [4–6]. So far, the
38 incorporation of PLA and bio-fillers has been reported to be an efficient and useful
39 approach to develop relatively inexpensive biocomposites with superior characteristics
40 [7,8], such as strength [9,10], flame retardancy [11,12], thermal stability [13], gas barrier
41 [14]. Some of these biocomposites have been successfully applied in the field of
42 packaging, textile sectors, medical devices, and others owing to the improved
43 compatibility between hydrophilic biopolymers and hydrophobic PLA polymer matrix
44 [2].

45 Condensed tannins, composed of flavonoid units, are one of the most abundant and
46 sustainable biopolymers in the plant. Figure 1 displays a simple flavonoid structure,
47 which represents four main structure of flavonoid units in condensed tannin. Their
48 characteristics like antioxidant, antimicrobial and stabilizing properties are attracting for
49 polymer materials. It has been shown that tannins displayed antioxidant and UV-
50 protective properties on polypropylene [15,16], polyethylene [17], poly (vinyl chloride)
51 (PVC) [18], and polyvinyl alcohol [19]. Recently, a study reported the incorporation of
52 tannins and PLA [20]. However, the presence of highly polarized hydroxyl groups in
53 tannin molecules makes it difficult to achieve good compatibility due to the low polarity
54 PLA matrix, resulting in poor interfacial adhesion and dispersion of tannin in the PLA
55 matrix. Esterification and hydroxypropylation of tannin have performed in order to
56 increase the compatibility and the dispersion capacity with various plastic matrix [21–
57 26], guaranteeing successful applications like carbon fiber precursors [22] or
58 functionalized composites [23]. However, a series of complex pretreated processes,
59 involving long-term chemical reaction, precipitation, filtration, and purification, should

60 be performed before compounding with a polymer matrix. Hence efficient and cost
61 effective modification and continuous processing techniques are required for exploring
62 more possible applications with a competitive prices. Inspired by the chemical reactivity
63 of tannins, it is possible to improve the interfacial adhesion of PLA-tannin via one-step
64 compatibilization approach with suitable compatibilizers/coupling agents [27,28].



65

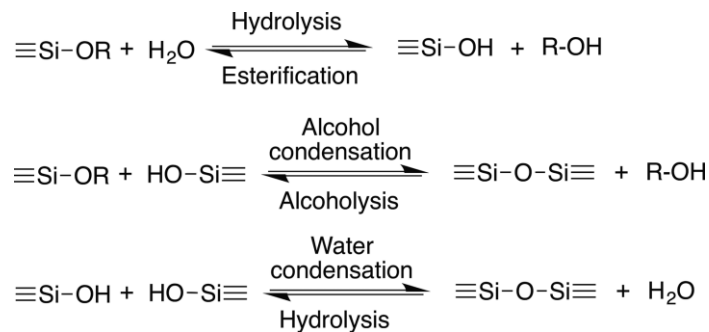
66 *Figure 1. Simple structure of flavonoid unit of condensed tannins*

67 One-step compatibilization is a well documented approach to develop composites
68 with good compatibilization [29–32], through which chemical reaction occurs between
69 each component during the melt blending process with the help of adhesion promoters
70 (e.g. coupling agents, compatibilizers) [2,29]. Hence, this method can promote the
71 interfacial adhesion of components and consequently the dispersion of the fillers in the
72 polymer matrix during melt extrusion [33,34]. However, only few literature reports have
73 addressed biocomposites prepared via reactive extrusion in one step [35,36].

74 Isocyanate derivatives are widely used as adhesion promoters to improve the
75 interface between PLA and biofillers because isocyanate group is highly reactive towards
76 hydroxyl moieties, yielding a urethane linkage between the polymer and natural fillers
77 [37–40]. As a result, composites based on a high content of lignin (up to 65%) and
78 polybutylene succinate (PBS) using polymeric methylene diphenyl diisocyanate as a
79 compatibilizer were prepared via melt mixing process and displayed an improved
80 interfacial adhesion [41]. Tannins containing various hydroxyl groups and PLA chains
81 bearing functional end-extremities (e.g. hydroxyl and carboxylic acid), can both react
82 with diisocyanate [27,28]. García [42] reported the utilization of polymeric methyl

83 diisocyanate to improve the compatibility between hydroxypropyl tannin and PLA
 84 matrix through a polymerization during the melt-blending in a rheometer chamber. The
 85 **crosslinking-grafting reaction** during the melt-blending was evidenced by the carbamate
 86 moiety (R1–O–CO–NH–R2) identified by the FTIR analysis and a typical fluorescence
 87 pattern detected by confocal microscopy. Thus, isocyanates can be utilized to enhance
 88 the compatibility of hydrophilic tannin with hydrophobic PLA.

89 The phenolic hydroxyl groups of tannins can easily react with amine even at room
 90 temperature [43–46]. On this basis, silane bearing amine functional groups could be a
 91 suitable adhesion promoter for processing polymeric composites containing tannin. The
 92 work of Zhu reported that the mechanical properties of flax/tannin composites were
 93 boosted by aminopropyltriethoxysilane (APS) [47]. Amino-silanes are commonly found to
 94 improve the interfacial bonding of biofillers containing numerous hydroxyl groups (e.g.
 95 fiber, flax, wood flour) and PLA matrix [48–51]. According to the work of Lu and co-
 96 workers, the primary amine group of APS can react with PLA via ammonolysis to form
 97 covalent bonding between cellulose and PLA under mild conditions [48]. The hydrolysis
 98 and condensation reaction of alkoxy silanes are shown in Figure 2. Under suitable
 99 conditions, silanes undergo hydrolysis, alcohol condensation, and/or water
 100 condensation to create Si-O-Si bonds. Based on this mechanism, Meng created a super
 101 tough PLA-silane nanohybrids via in situ crosslinking PLA-silanes [52]. Amino-silane was
 102 also reported to improve the interfacial interaction of PLA-nanocellulose based on the
 103 successful silane grafting of PLA via melt blending [50]. Therefore, amino-silanes were
 104 supposed to improve the interfacial adhesion of PLA-tannin via **reactive extrusion**.



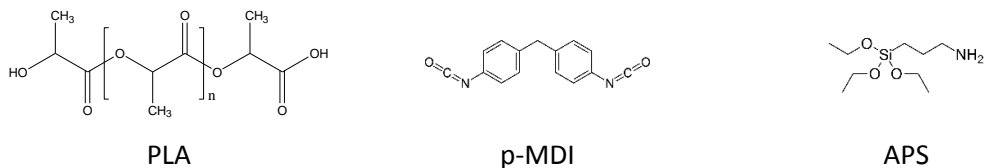
105
 106 *Figure 2. Hydrolysis and condensation reactions of alkoxy silanes [52]*

107 Inspired by those previous studies, we report here a simple one-step efficient
108 method to improve the compatibility between PLA and tannin via reactive extrusion.
109 Methylene diphenyl diisocyanate (p-MDI) and 3-aminopropytriethoxysilane (APS) were
110 chosen as adhesion promoters. The final composites were characterized by tensile,
111 morphological, rheological, and thermal properties.

112 2. Materials and Methods

113 2.1. Materials

114 PLA trademarked under the name of Ingeo™ Biopolymer (Grade 3D850), was
115 obtained from Natureworks LLC (Minnesota, USA). Mimosa tannins were purchased
116 from Silva Chimica, in Mondovi, Italy. Methylene diphenyl diisocyanate (p-MDI) was
117 used as a compatibilizer, which is a commercial resin with 57% polyisocyanates content
118 fabricated by Bayer. Silane coupling agent (3-aminopropytriethoxysilane, APS, 98%) was
119 obtained from Alfa Aesar. The chemical structures of the used chemicals and PLA are
120 presented in Figure 3.



121 *Figure 3. Chemical structures of PLA, p-MDI, and APS*

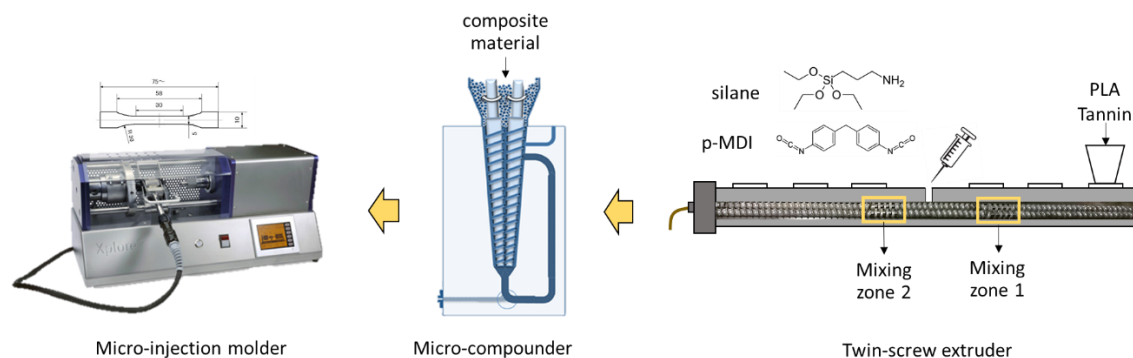
122 2.2. Preparation of PLA/tannin composites

123 PLA was ground into powder by a grinder for better mixing with tannin. PLA and
124 tannin (T) powder were oven-dried at 80°C for more than 12 hours to eliminate possible
125 absorbed water on the surface. The blending ratio of PLA and T was 90/10 (w/w). The
126 silane was fed directly via syringe, while p-MDI was diluted with acetone (p-MDI:
127 acetone=75:25 v/v) to reduce the viscosity before injection.

128 The blending of PLA and T was carried out in a twin-screw extruder (Thermo
129 Scientific™ Process 11, Villebon-sur-Yvette, France). The temperature of the die and the
130 heating zones across the extruder barrel are shown in *Table 1*. The screw speed was 100

131 rpm and the residence time was 4 min approximately. In the current experiment, the
 132 screw profile was designed two mixing zones for obtaining effective mixing perform:
 133 zone 1 designed before the addition of compatibilizer for premixing PLA and tannin,
 134 while zone 2 aimed to guarantee well blend with compatibilizer. The adhesion
 135 promoters were fed by using a syringe, the injecting speed was controlled by a syringe
 136 pump (WPI, SP120PZ, MA, USA). The flow rate of PLA/T powder was 6.6 g/min while the
 137 flow rate speed of the silane and p-MDI was 0.8 g/min and 1 g/min, respectively, to
 138 ensure the ratio of compatibilizer was approximately 12%. The PLA/tannin blend
 139 without compatibilizer noted as PLT, while with silane and p-MDI were named as PLTSi
 140 and PLTM, respectively.

141 The extruded composite materials were ground into small particles by a grinder for
 142 further use. The tensile test specimens (dumbbell-shaped, ISO 527, type 1A) were
 143 carried out by a micro-compounder (Micro 15, DSM Xplore, Sittard, Netherlands) and a
 144 micro-injection molder (Xplore, Sittard, Netherlands).



145

146 *Figure 4. From right to left: reactive extrusion using a twin-screw extruder, the specimens*
 147 *molding process by micro-compounder and micro-injection molder.*

Table 1. Temperature of screw profile

Zone	die	8	7	6	5	4	3	2	1
T (°C)	185	155	180	190	190	190	200	200	200

148 2.3. Characterizations

149 The tensile test was performed at room temperature on Instron tensile testing

150 machine (model 5569, Norwood, MA, USA) equipped with a 50 kN load cell. The cross-
151 head speed used was of 1 mm/min according to EN ISO 527:1996. Four replicates were
152 tested for each sample to obtain an average value.

153 The morphology of fracture surface after the tensile test was characterized by a
154 scanning electron microscopy (SEM, JSM-6490LV, Tokyo, JAPAN) with an acceleration
155 voltage of 5kV. All the samples were coated with a thin layer of gold by using a Polaron
156 SEM coating system (SC7620, Hertfordshire, England) for 5 min at a current between 4
157 and 5 mA.

158 Rheological properties of PLA/tannin composites were analyzed on a rheometer (TA
159 instrument, G2 ARES, New Castle, DE, USA) using a parallel-plate geometry (25 mm
160 diameter, 1 mm gap) under a nitrogen atmosphere, in order to prevent thermo-
161 oxidative degradation. Dynamic strain sweep tests to determine the linear viscoelastic
162 region (LVR) was realized at 1 rad/s, in a range of 0.1-1000%, resulting in a strain applied
163 of 10% chosen for frequency tests. Dynamic frequency sweep tests were performed
164 over an angular frequency range of 0.1-623.3 rad/s at 190°C.

165 The Differential scanning calorimetry (DSC) analysis was carried out using a Mettler
166 Toledo DSC 1 (Columbus, Ohio, USA) with a scan rate of 10°C/min within the
167 temperature range of 30°C to 220°C and 220°C to -10°C in the second scanning cycle. A
168 total sample weight 3-4 mg was used for measurement in a aluminum pan under a
169 nitrogen atmosphere (50 mL/min). Melting temperatures (T_m), enthalpy of melting
170 (ΔH_m) and cold crystallization (ΔH_c) were analyzed by STARE evaluation software
171 (version 10.00). ΔH_m^0 is the enthalpy of melting 100% crystallized PLA, which is equal to
172 93.7 J/g [53], and w is the weight fraction of PLA. The percentage crystallinity X_c (%) was
173 estimated by the following equation (1):

174
$$X_c(\%) = \frac{\Delta H_m - \Delta H_c}{\Delta H_m^0 \times w} \times 100\% \quad (1)$$

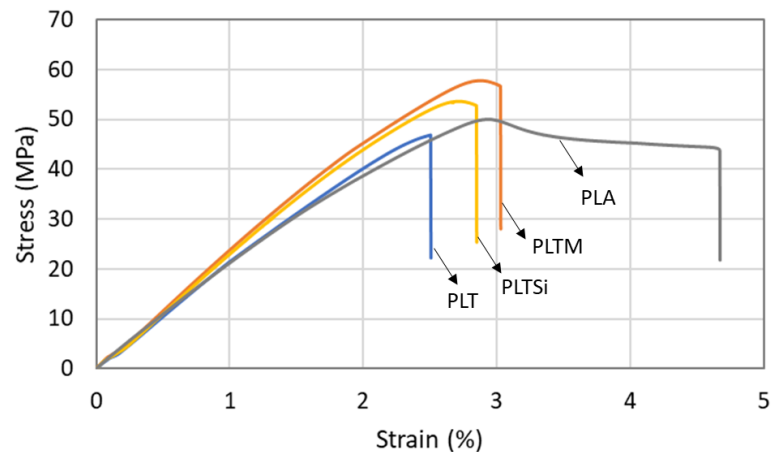
175 Thermogravimetric analysis (TGA) was performed by using a Mettler Toledo TGA/DSC
176 (Columbus, Ohio, USA). The samples with a total weight in the 6–7 mg range were
177 scanned in the range of 30-600°C with a heating rate 10°C/min in an air atmosphere (50

178 mL/min). The obtained data were analyzed by STARE evaluation software (version
179 10.00).

180 3. Results and discussion

181 3.1. Tensile property

182 Figure 5 presents the strain-stress curves of PLA/tannin composite with or without
183 adhesion promoters and related data was given in table 2. Compared with PLA,
184 PLA/tannin composite without adhesion promoters (PLT) presented a comparable
185 Young's modulus but a lower tensile strength due to the weak interfacial adhesion of
186 PLA-tannin. With the addition of a compatibilizer (PLTM or PLTSi), an increase of both
187 Young's moduli and tensile strengths were observed. For thermoplastic composite
188 materials, Young's moduli are generally improved by adding a filler because the filled
189 components restrict the chain mobility of the polymer chain [54]. The tensile strength of
190 PLTM and PLTSi are 19.1% and 12.8% higher than that of PLT, respectively, referring to
191 better interfacial adhesion between tannin and PLA matrix. While the elongation of
192 PLA/tannin blends was observed a decrease without exception compared with neat PLA
193 since lack of plasticizers to release the stress concentration between the interface of
194 tannin and PLA [55]. These results are in agreement with the work of García [42].



195

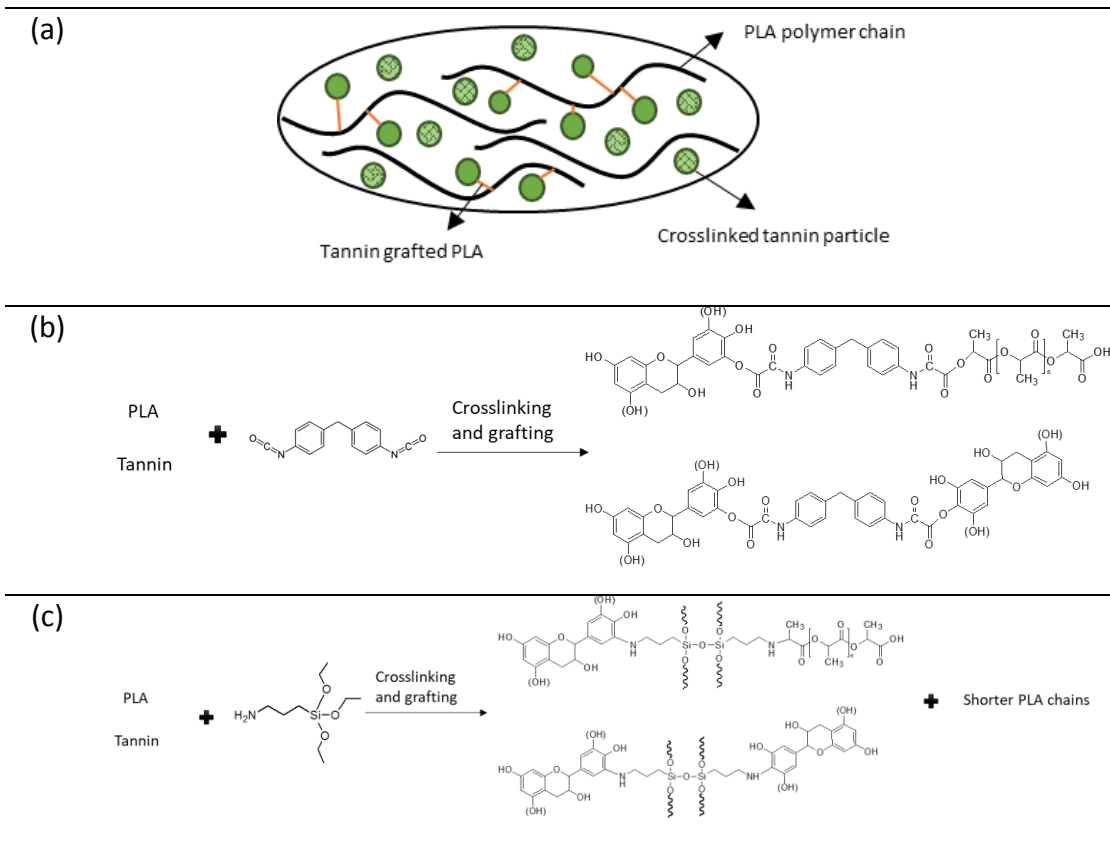
196 **Figure 5. Strain-stress curves of PLA/tannin composites**

197 **Table 2. Main tensile properties of PLA/tannin composites**

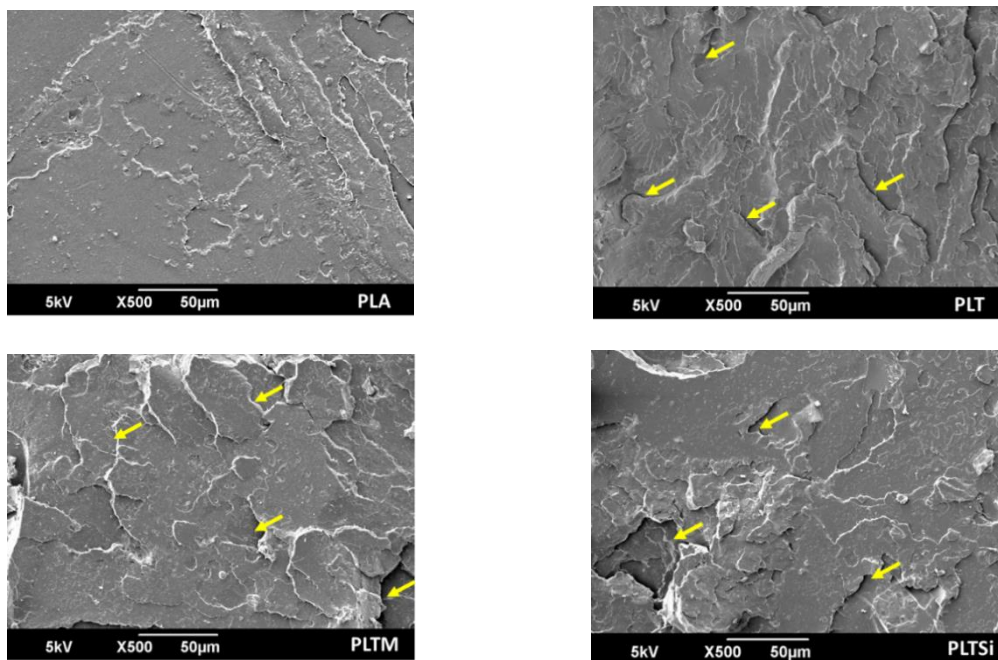
Sample	Young's modulus (GPa)	tensile strength (MPa)	Elongation (%)
PLA	3.5±0.1	50±1	4.7±0.5
PLT	3.5±0.3	47±3	2.5±0.2
PLTM	3.9±0.3	56±1	3.0±0.2
PLTSi	3.8±0.3	53±1	2.8±0.1

198 The changes of tensile property can be explained by the interaction of PLA, tannin,
199 and p-MDI/Silane, forming crosslinked tannin particles and/or local crosslinking and
200 interpenetrating network structure of tannin-PLA during the melt blending process. The
201 proposed representative microstructure of PLA/tannin composites compatibilized by p-
202 MDI/APS was represented in Scheme 1 (a) and all possible reactions have been listed in
203 Scheme 1 (b-c). Taking into account the well known high reactivity of tannins with
204 nucleophilic reagents in general and the reaction of PLA by both hydroxyl and carboxylic
205 acid groups with isocyanates under mild conditions [56]. The **chemical reaction** of PLA
206 and tannin was achieved using p-MDI via melt-blending as reported by García and his
207 colleagues Scheme 1 (b)) [42]. For silane coupling agent, PLA and tannin were proposed
208 to crosslink with APS through electrophilic substitution and / or ester-amide exchange
209 reaction (Scheme 1 (c)) [48,52]. In the blending system, tannin was proposed to
210 crosslink with p-MDI/APS leading to the formation of stiff thermoset particles, these
211 particles will be dispersed in the PLA matrix as internal crosslinked domains. Considering
212 that these particles are still functionalized with a variety of reactive function groups
213 thereby it will act further as local crosslinking points to connect the chains of PLA. Thus,
214 the **crosslinking-grafting reactions** between PLA, tannin and p-MDI/APS created a
215 complicated network, with upgraded interfacial adhesion and remarkable stress transfer
216 between the two phases. This contributes to the improvement of tensile strength
217 compared with PLT.

218 *Scheme 1. The proposed representative microstructure of PLA/tannin composites and illustration*
219 *of the proposed crosslinking-grafting reactions between PLA, tannin and p-MDI/APS*



220 The morphology of tensile-fracture surface of each sample was observed by SEM
 221 microscopy and the SEM micrographs are displayed in Figure 6. The fracture surface of
 222 PLA is relatively smooth and PLA/tannin composites present a distinct coarse fracture
 223 surface. Similar with the study of Answer et al [20], it is difficult to identify tannin
 224 particles between PLA and tannin since tannin was generally wetted by PLA matrix. The
 225 coarse region of PLA-tannin blends is the deboned interface (marked in yellow arrows)
 226 at regions of higher stress intensity during fracture. From these areas, composites with
 227 compatibilizer displayed tougher and deeper interfacial gaps compared with native
 228 PLA/tannin composite, referring a stronger interfacial adhesion between filler and
 229 polymer matrix. Similar phenomena can be found in the PLA/starch composites
 230 compatibilized by isocyanate [38] and chemical crosslinked PLA [53].

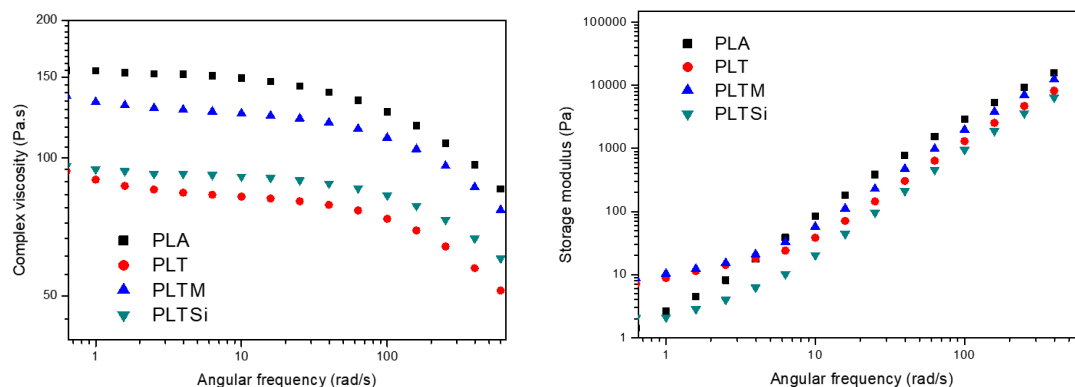


231 *Figure 6. SEM micrographs of the tensile-fracture surface of PLA and PLA/tannin composites.*

232 **3.2. Rheological property**

233 The measurement of rheological properties of polymeric materials under the molten
 234 state is useful to detect changes in the molecular structure via a one-step
 235 compatibilization process. The complex viscosity and storage modulus were used to
 236 explore the flow behavior as a result of all acting interactions in PLA-tannin composites.
 237 As presented in Figure 7, complex viscosity in all curves decreased as a function of
 238 angular frequency, exhibiting a typical shear-thinning behavior. The introduction of
 239 tannin in PLA results in a sharply decrease of complex viscosity because of poor
 240 interfacial adhesion between PLA and tannin and absence of uniform distribution.
 241 However, PLA/tannin composite compatibilized with APS or p-MDI (PLTSi or PLTM)
 242 displayed an enhanced complex viscosities compared with incompatibilized composite
 243 (PLT), suggesting the formation of bonding between tannin and PLA polymer chain
 244 and/or crosslink of tannin (see Scheme 1). This increase in complex viscosity is
 245 particularly marked for PLTM and with the association of improved tensile strength and
 246 tougher tensile-fracture surface, indicating a stronger interfacial adhesion between two
 247 components. As previously described for filled polymer systems, a plateau-like behavior

248 of storage modulus was observed in all PLA/tannin composites at low frequency (<5
249 rad/s), suggesting that the presence of tannin limited the mobility of polymer chains and
250 reinforced the internal network structure [57,58]. For PPTM and PPTSi, the network
251 structure created by the crosslinking-grafting reaction of PLA could also contribute to
252 such plateau-like behavior. PLTSi exhibited lower complex viscosity and storage modulus
253 compared with PLTM since the reaction between APS and PLA generated shorter chain
254 since the amine group on APS reacted with PLA through ester-amide exchange
255 reactions, resulting in chain scission [52], see Scheme 1 (c). These results are in
256 accordance with the work of Meng [52].

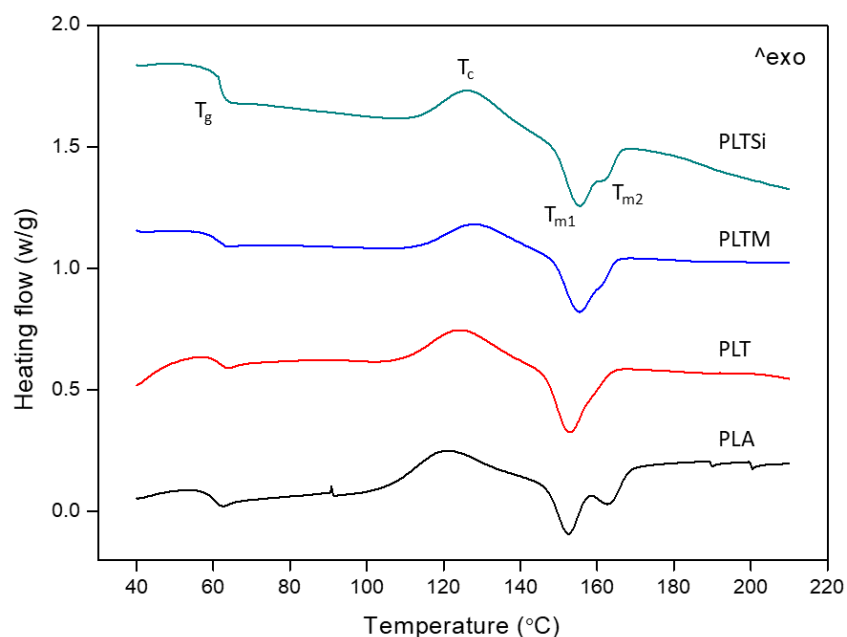


257 *Figure 7. Rheological behavior of PLA and PLA/tannin composites*

258 3.3. Crystallization and melting behavior

259 The effect of tannin and compatibilizers on the glass transition temperature,
260 crystallization and melting behavior of PLA and PLA/tannin composites were
261 characterized by differential scanning calorimetry (DSC), and are shown in Figure 8. The
262 related results from the second heat-cool circle are given in Table 3. All samples
263 displayed clear glass transition, cooling crystallization and melting peak. Compared with
264 PLA, a slight shift to a higher temperature for T_g and T_c of PLA/tannin composites was
265 observed indicating a decrease in the mobility of polymer molecules in the vicinity of the
266 interface [59]. This is generally found in the blends of PLA and bio-fillers even without
267 compatibilizers, such as starch [4], cellulose [50], coconut shell powder [51], etc. PLA
268 exhibited two obvious melting peaks revealing two kinds of lamellae structure. The low-
269 melting peak is attributed to an imperfect crystal structure, while the high-melting peak

270 refers to a more orderly crystal structure [60]. The addition of tannin inhibited the
 271 crystallization of PLA, thus, PLT has a broad melting enthalpy and the crystallinity of PLA
 272 disappeared. However, T_m of PLA/tannin composites shifts to a higher temperature by
 273 adding p-MDI or APS, referring to an improvement of the interfacial interaction between
 274 tannin and PLA matrix. Similar results can be found in PLA biocomposites compatibilized
 275 by either isocyanates [38,42,61,62] or silanes [50,63]. The crosslinking structure in PLA
 276 polymer may also inhibit chain segments motion for crystallization [53], thus, a decrease
 277 of X_c can be found in PLTM and PLTSi.



278

279 *Figure 8. DSC thermograms of PLA and PLA/tannin composites*

280

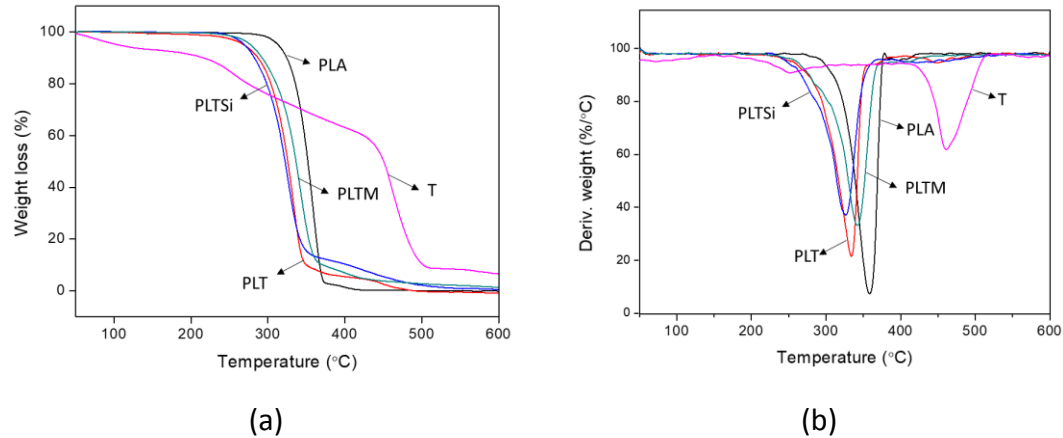
Table 3. DSC data of PLA and PLA/tannin composites

Sample	T_g (°C)	ΔH_c (J/g)	T_c (°C)	ΔH_m (J/g)	$T_{m1}; T_{m2}$ (°C)	X_c (%)
PLA	55.9	14.0	120.4	20.7	152.5;162.9	8.0
PLT	58.6	17.8	125.2	14.7	152.8	--
PLTM	57.2	9.6	128.0	15.7	155.3;161.4	7.3
PLTSi	60.0	15.9	126.8	17.0	155.4;161.9	1.2

Note: no crystallinity: --.

281 **3.4. Thermal property**

282 The thermal degradation behavior of tannin, PLA and PLA/tannin blends was
283 determined by thermogravimetric analyses in an air atmosphere. Their weight losses as
284 a function of temperature and differential thermal gravity (DTG) data are presented in
285 Figure 9. Tannin exhibits a three-step degradation process, which include the loss of
286 adsorbed water, the decomposition of linkage between flavonoid units and pyrolytic
287 degradation [64]. PLA and PLA/tannin blends showed a one-step degradation process,
288 which was represented by a single peak as shown in the DTG curves, while char
289 formation can be observed with the addition of tannin at high temperature (~350°C)
290 during the pyrolysis process. The char acts as a protective barrier that can suppress the
291 thermal decomposition of the PLA matrix [51]. Tannin results in a lower onset
292 decomposition temperature which can be explained by the reduction of crystallinity of
293 PLA/tannin blends. Besides, the decomposition process of composites also relies on the
294 thermal stability of each component, interfacial adhesion between the two components
295 and molecular weight of the polymer matrix [38,42]. The higher decomposition
296 temperature of PLTM can be further confirmed the improvement of interfacial
297 adhesion, which can be found PLA/biopolymer composites compatibilized with
298 isocyanate [38,61]. In accordance with Meng [52], the decomposition temperature of
299 PLTSi is close to that of PLT, probably due to ester-amide exchange reactions of PLA and
300 APS, causing chain scissions. The higher residues of PLTSi and PLTM at a high
301 temperature can be rationalized by the crosslinked network between PLA and tannin.



302 **Figure 9. Thermal analysis profile of PLA and PLA/tannins composites: (a) TGA curves; (b) DTG**
 303 **curves.**

304 **4. Conclusions**

305 PLA/tannin biocomposite showing good compatibility can be successfully processed
 306 via one-step reactive extrusion with the help of p-MDI or APS. The compatibilized
 307 composites acquire a stronger interfacial adhesion between PLA and tannin, leading to
 308 superior tensile strength and Young's modulus compared with incompatibilized
 309 PLA/tannin composite. The compatibilized composites acquire a stronger interfacial
 310 adhesion between PLA and tannin, leading to superior tensile strength and Young's
 311 modulus compared with incompatibilized PLA/tannin composite. Moreover, higher
 312 melting temperature and onset of thermal degradation of resulting composite
 313 evidenced an elevated capacity for compatibility using p-MDI. Thus, this approach could
 314 be applied to efficiently prepare similar PLA-based biocomposites.

315
 316 **Acknowledgements**

317 This work was supported by the National Natural Science Foundation of China
 318 (NSFC 31760187, 31971595) and Natural Science Foundation of Yunnan (2017FB060) as
 319 well as the Yunnan provincial youth and middle-age reserve talents of academic and
 320 technical leaders (2019HB026). LERMAB is supported by the French National Research
 321 Agency through the Laboratory of Excellence ARBRE (ANR-12-LABXARBRE-01). Pascal
 322 Xanthopoulos and Polybridge® are thanked fruitful discussions. **Financial support from**

323 China Scholarship Council is gratefully acknowledged. The authors also thank Richard
324 Laine for precious technical support and Philippe Marchal for the guidance of rheology
325 experiment.

326

327

328 **5. References**

- 329 [1] M.L. Di Lorenzo, R. Androsch, M.A. Abdel-Rahman, eds., *Synthesis, structure and*
330 *properties of poly(lactic acid)*, Springer, Cham, Switzerland, 2018.
- 331 [2] D. Ray, ed., *Biocomposites for high-performance applications: current barriers and*
332 *future needs towards industrial development*, Woodhead Publishing, an imprint of
333 Elsevier, Duxford, United Kingdom, 2017.
- 334 [3] K. Formela, Ł. Zedler, A. Hejna, A. Tercjak, *Reactive extrusion of bio-based polymer*
335 *blends and composites – Current trends and future developments*, *EXPRESS Polym.*
336 *Lett.* 12 (2018) 24–57. <https://doi.org/10.3144/expresspolymlett.2018.4>.
- 337 [4] Y. feng Zuo, J. Gu, Z. Qiao, H. Tan, J. Cao, Y. Zhang, *Effects of dry method*
338 *esterification of starch on the degradation characteristics of starch/poly(lactic acid)*
339 *composites*, *Int. J. Biol. Macromol.* 72 (2015) 391–402.
340 <https://doi.org/10.1016/j.ijbiomac.2014.08.038>.
- 341 [5] S. Lv, Y. Zhang, J. Gu, H. Tan, *Biodegradation behavior and modelling of soil burial*
342 *effect on degradation rate of PLA blended with starch and wood flour*, *Colloids Surf.*
343 *B Biointerfaces.* 159 (2017) 800–808.
344 <https://doi.org/10.1016/j.colsurfb.2017.08.056>.
- 345 [6] K. Jha, R. Kataria, J. Verma, S. Pradhan, *Potential biodegradable matrices and fiber*
346 *treatment for green composites: A review*, *Mater.* 2019 Vol 6 Pages 119-138.
347 (2019). <https://doi.org/10.3934/matersci.2019.1.119>.
- 348 [7] A. Basu, M. Nazarkovsky, R. Ghadi, W. Khan, A.J. Domb, *Poly(lactic acid)-based*
349 *nanocomposites*, *Polym. Adv. Technol.* 28 (2017) 919–930.
350 <https://doi.org/10.1002/pat.3985>.
- 351 [8] C. Wang, S.S. Kelley, R.A. Venditti, *Lignin-Based Thermoplastic Materials*,
352 *ChemSusChem.* 9 (2016) 770–783. <https://doi.org/10.1002/cssc.201501531>.
- 353 [9] L. Wan, S. Zhou, Y. Zhang, *Parallel advances in improving mechanical properties*
354 *and accelerating degradation to poly(lactic acid)*, *Int. J. Biol. Macromol.* 125 (2019)
355 1093–1102. <https://doi.org/10.1016/j.ijbiomac.2018.12.148>.
- 356 [10] L. Wan, Y. Zhang, *Jointly modified mechanical properties and accelerated*
357 *hydrolytic degradation of PLA by interface reinforcement of PLA-WF*, *J. Mech.*
358 *Behav. Biomed. Mater.* 88 (2018) 223–230.
359 <https://doi.org/10.1016/j.jmbbm.2018.08.016>.
- 360 [11] F. Laoutid, V. Karaseva, L. Costes, S. Brohez, R. Mincheva, P. Dubois, *Novel Bio-*
361 *based Flame Retardant Systems Derived from Tannic Acid*, *J. Renew. Mater.* 6
362 (2018) 559–572. <https://doi.org/10.32604/JRM.2018.00004>.
- 363 [12] F. Laoutid, H. Vahabi, M. Shabanian, F. Aryanasab, P. Zarrintaj, M.R. Saeb, *A new*
364 *direction in design of bio-based flame retardants for poly(lactic acid)*, *Fire Mater.*
365 42 (2018) 914–924. <https://doi.org/10.1002/fam.2646>.
- 366 [13] A. Kumar, V.R. Tumu, S. Ray Chowdhury, R.R. S.V.S., *A green physical approach to*
367 *compatibilize a bio-based poly (lactic acid)/lignin blend for better mechanical,*
368 *thermal and degradation properties*, *Int. J. Biol. Macromol.* 121 (2019) 588–600.
369 <https://doi.org/10.1016/j.ijbiomac.2018.10.057>.
- 370 [14] S.S. Karkhanis, N.M. Stark, R.C. Sabo, L.M. Matuana, *Water vapor and oxygen*

371 barrier properties of extrusion-blown poly(lactic acid)/cellulose nanocrystals
372 nanocomposite films, *Compos. Part Appl. Sci. Manuf.* 114 (2018) 204–211.
373 <https://doi.org/10.1016/j.compositesa.2018.08.025>.

374 [15] J. Liao, N. Brosse, A. Pizzi, S. Hoppe, Dynamically Cross-Linked Tannin as a
375 Reinforcement of Polypropylene and UV Protection Properties, *Polymers*. 11 (2019)
376 102. <https://doi.org/10.3390/polym11010102>.

377 [16] J. Liao, N. Brosse, A. Pizzi, S. Hoppe, X. Xi, X. Zhou, Polypropylene Blend with
378 Polyphenols through Dynamic Vulcanization: Mechanical, Rheological, Crystalline,
379 Thermal, and UV Protective Property, *Polymers*. 11 (2019) 1108.
380 <https://doi.org/10.3390/polym11071108>.

381 [17] J. Bridson, J. Kaur, Z. Zhang, L. Donaldson, A. Fernyhough, Polymeric flavonoids
382 processed with co-polymers as UV and thermal stabilisers for polyethylene films,
383 *Polym Degrad Stabil.* 122 (2015) 18–24.
384 <https://doi.org/10.1016/j.polymdegradstab.2015.10.002>.

385 [18] H. Shnawa, M. Khaleel, F. Muhamed, Oxidation of HDPE in the Presence of PVC
386 Grafted with Natural Polyphenols (Tannins) as Antioxidant, *J. Polym. Chem.* 05
387 (2015) 9–16. <https://doi.org/10.4236/ojpcem.2015.52002>.

388 [19] Y. Zhai, J. Wang, H. Wang, T. Song, W. Hu, S. Li, Preparation and Characterization of
389 Antioxidative and UV-Protective Larch Bark Tannin/PVA Composite Membranes,
390 *Molecules*. 23 (2018) 2073. <https://doi.org/10.3390/molecules23082073>.

391 [20] M. Anwer, H.E. Naguib, A. Celzard, V. Fierro, Comparison of the thermal, dynamic
392 mechanical and morphological properties of PLA-Lignin & PLA-Tannin particulate
393 green composites, *Compos Part B Eng.* 82 (2015) 92–99.
394 <https://doi.org/10.1016/j.compositesb.2015.08.028>.

395 [21] D.E. García, W.G. Glasser, A. Pizzi, S. Paczkowski, M.-P. Laborie, Hydroxypropyl
396 tannin from *Pinus pinaster* bark as polyol source in urethane chemistry, *Eur. Polym.*
397 *J.* 67 (2015) 152–165. <https://doi.org/10.1016/j.eurpolymj.2015.03.039>.

398 [22] W. Grigsby, J. Kadla, Evaluating Poly(lactic acid) Fiber Reinforcement with Modified
399 Tannins, *Macromol Mater Eng.* 299 (2014) 368–378.
400 <https://doi.org/10.1002/mame.201300174>.

401 [23] W. Grigsby, J. Bridson, C. Lomas, H. Frey, Evaluating Modified Tannin Esters as
402 Functional Additives in Polypropylene and Biodegradable Aliphatic Polyester,
403 *Macromol Mater Eng.* 299 (2014) 1251–1258.
404 <https://doi.org/10.1002/mame.201400051>.

405 [24] M. Gaugler, W. Grigsby, D. Harper, T. Rials, Chemical imaging of the spatial
406 distribution and interactions of tannin dispersal in bioplastic systems, *Adv. Mater.*
407 *Res.* 29–30 (2007) 173–176. <https://doi.org/10.4028/www.scientific.net/AMR.29-30.173>.

408
409 [25] W.J. Grigsby, J.H. Bridson, C. Schrade, Modifying biodegradable plastics with
410 additives based on condensed tannin esters, *J Appl Polym Sci.* 132 (2015) 41626.
411 <https://doi.org/10.1002/app.41626>.

412 [26] W.J. Grigsby, J.H. Bridson, C. Lomas, J.-A. Elliot, Esterification of Condensed Tannins
413 and Their Impact on the Properties of Poly(Lactic Acid), *Polymers*. 5 (2013) 344–
414 360. <https://doi.org/10.3390/polym5020344>.

- 415 [27] A. Pizzi, Tannin-Based Adhesives, *J. Macromol. Sci. Part C.* 18 (1980) 247–315.
416 <https://doi.org/10.1080/00222358008081043>.
- 417 [28] A. Arbenz, L. Avérous, Chemical modification of tannins to elaborate aromatic
418 biobased macromolecular architectures, 17 (2015) 2626–2646.
419 <https://doi.org/10.1039/C5GC00282F>.
- 420 [29] B. Wang, L. Hao, W. Wang, G. Hu, One-step compatibilization of polyamide 6/ poly
421 (ethylene-1-octene) blends with maleic anhydride and peroxide, *J. Polym. Res.* 17
422 (2010) 821–826. <https://doi.org/10.1007/s10965-009-9373-9>.
- 423 [30] G.-H. Hu, H. Cartier, L.-F. Feng, B.-G. Li, Kinetics of the in situ polymerization and in
424 situ compatibilization of poly(propylene) and polyamide 6 blends, *J. Appl. Polym.*
425 *Sci.* 91 (2004) 1498–1504. <https://doi.org/10.1002/app.13329>.
- 426 [31] X. Xie, X. Zheng, Effect of addition of multifunctional monomers on one-step
427 reactive extrusion of PP/PS blends, *Mater. Des.* 22 (2001) 11–14.
428 [https://doi.org/10.1016/S0261-3069\(00\)00028-5](https://doi.org/10.1016/S0261-3069(00)00028-5).
- 429 [32] Y. Pietrasanta, J.-J. Robin, N. Torres, B. Boutevin, Reactive compatibilization of
430 HDPE/PET blends by glycidyl methacrylate functionalized polyolefins, *Macromol.*
431 *Chem. Phys.* 200 (1999) 142–149. [https://doi.org/10.1002/\(SICI\)1521-3935\(19990101\)200:1<142::AID-MACP142>3.0.CO;2-W](https://doi.org/10.1002/(SICI)1521-3935(19990101)200:1<142::AID-MACP142>3.0.CO;2-W).
- 433 [33] C. Nyambo, A.K. Mohanty, M. Misra, Effect of Maleated Compatibilizer on
434 Performance of PLA/Wheat Straw-Based Green Composites, *Macromol. Mater. Eng.*
435 296 (2011) 710–718. <https://doi.org/10.1002/mame.201000403>.
- 436 [34] M.E. González-López, J.R. Robledo-Ortíz, R. Manríquez-González, J.A. Silva-Guzmán,
437 A.A. Pérez-Fonseca, Polylactic acid functionalization with maleic anhydride and its
438 use as coupling agent in natural fiber biocomposites: a review, *Compos. Interfaces.*
439 25 (2018) 515–538. <https://doi.org/10.1080/09276440.2018.1439622>.
- 440 [35] M.-B. Coltelli, N. Mallegni, S. Rizzo, P. Cinelli, A. Lazzeri, Improved Impact
441 Properties in Poly(lactic acid) (PLA) Blends Containing Cellulose Acetate (CA)
442 Prepared by Reactive Extrusion, *Materials.* 12 (2019) 270.
443 <https://doi.org/10.3390/ma12020270>.
- 444 [36] L. Quiles-Carrillo, N. Montanes, C. Sammon, R. Balart, S. Torres-Giner,
445 Compatibilization of highly sustainable polylactide/almond shell flour composites
446 by reactive extrusion with maleinized linseed oil, *Ind. Crops Prod.* 111 (2018) 878–
447 888. <https://doi.org/10.1016/j.indcrop.2017.10.062>.
- 448 [37] H. Wang, X. Sun, P. Seib, Mechanical properties of poly(lactic acid) and wheat
449 starch blends with methylenediphenyl diisocyanate, *J. Appl. Polym. Sci.* 84 (2002)
450 1257–1262. <https://doi.org/10.1002/app.10457>.
- 451 [38] L. Yu, E. Petinakis, K. Dean, H. Liu, Q. Yuan, Enhancing compatibilizer function by
452 controlled distribution in hydrophobic polylactic acid/hydrophilic starch blends, *J.*
453 *Appl. Polym. Sci.* 119 (2011) 2189–2195. <https://doi.org/10.1002/app.32949>.
- 454 [39] S. Krishnan, M. Smita, K.N. Sanjay, Renewable Resource based blends of Polylactic
455 acid (PLA) and Thermoplastic starch (TPS) using Novel Reactive Compatibilization -
456 ProQuest, *J. Polym. Mater.* 34 (2017) 525–538.
- 457 [40] B.-S. Baek, J.-W. Park, B.-H. Lee, H.-J. Kim, Development and Application of Green
458 Composites: Using Coffee Ground and Bamboo Flour, *J. Polym. Environ.* 21 (2013)

459 702–709. <https://doi.org/10.1007/s10924-013-0581-3>.

460 [41] S. Sahoo, M. Misra, A.K. Mohanty, Enhanced properties of lignin-based
461 biodegradable polymer composites using injection moulding process, *Compos. Part*
462 *Appl. Sci. Manuf.* 42 (2011) 1710–1718.
463 <https://doi.org/10.1016/j.compositesa.2011.07.025>.

464 [42] D.E. García, J.P. Salazar, S. Riquelme, N. Delgado, S. Paczkowski, Condensed Tannin-
465 Based Polyurethane as Functional Modifier of PLA-Composites, *Polym.-Plast.*
466 *Technol. Eng.* 57 (2018) 709–726.
467 <https://doi.org/10.1080/03602559.2017.1344855>.

468 [43] F. Braghiroli, V. Fierro, A. Pizzi, K. Rode, W. Radke, L. Delmotte, J. Parmentier, A.
469 Celzard, Reaction of condensed tannins with ammonia, *Ind. Crops Prod.* 44 (2013)
470 330–335. <https://doi.org/10.1016/j.indcrop.2012.11.024>.

471 [44] K. Kida, M. Suzuki, A. Takagaki, F. Nanjo, Deodorizing Effects of Tea Catechins on
472 Amines and Ammonia, *Biosci. Biotechnol. Biochem.* 66 (2002) 373–377.
473 <https://doi.org/10.1271/bbb.66.373>.

474 [45] K. Hashida, R. Makino, S. Ohara, Amination of pyrogallol nucleus of condensed
475 tannins and related polyphenols by ammonia water treatment, *Holzforschung.* 63
476 (2008) 319–326. <https://doi.org/10.1515/HF.2009.043>.

477 [46] M.C. Basso, C. Lacoste, A. Pizzi, E. Fredon, L. Delmotte, MALDI-TOF and ¹³C NMR
478 analysis of flexible films and lacquers derived from tannin, *Ind. Crops Prod.* 61
479 (2014) 352–360. <https://doi.org/10.1016/j.indcrop.2014.07.019>.

480 [47] J. Zhu, H. Zhu, K. Immonen, J. Brighton, H. Abhyankar, Improving mechanical
481 properties of novel flax/tannin composites through different chemical treatments,
482 *Ind. Crops Prod.* 67 (2015) 346–354. <https://doi.org/10.1016/j.indcrop.2015.01.052>.

483 [48] Y. Lu, M.C. Cueva, E. Lara-Curzio, S. Ozcan, Improved mechanical properties of
484 polylactide nanocomposites-reinforced with cellulose nanofibrils through
485 interfacial engineering via amine-functionalization, *Carbohydr. Polym.* 131 (2015)
486 208–217. <https://doi.org/10.1016/j.carbpol.2015.05.047>.

487 [49] P. Georgiopoulos, E. Kontou, G. Georgousis, Effect of silane treatment loading on
488 the flexural properties of PLA/flax unidirectional composites, *Compos. Commun.*
489 10 (2018) 6–10. <https://doi.org/10.1016/j.coco.2018.05.002>.

490 [50] M. Rahmat, M. Karrabi, I. Ghasemi, M. Zandi, H. Azizi, Silane crosslinking of
491 electrospun poly (lactic acid)/nanocrystalline cellulose bionanocomposite, *Mater.*
492 *Sci. Eng. C.* 68 (2016) 397–405. <https://doi.org/10.1016/j.msec.2016.05.111>.

493 [51] K.S. Chun, S. Husseinsyah, H. Osman, Mechanical and thermal properties of
494 coconut shell powder filled polylactic acid biocomposites: effects of the filler
495 content and silane coupling agent, *J. Polym. Res.* 19 (2012) 9859.
496 <https://doi.org/10.1007/s10965-012-9859-8>.

497 [52] X. Meng, N.A. Nguyen, H. Tekinalp, E. Lara-Curzio, S. Ozcan, Supertough PLA-Silane
498 Nanohybrids by in Situ Condensation and Grafting, *ACS Sustain. Chem. Eng.* 6 (2018)
499 1289–1298. <https://doi.org/10.1021/acssuschemeng.7b03650>.

500 [53] C. Yamoum, J. Maia, R. Magaraphan, Rheological and thermal behavior of PLA
501 modified by chemical crosslinking in the presence of ethoxylated bisphenol A
502 dimethacrylates: Rheological and Thermal Behaviors of PLA with Bis-EMA

503 Crosslinking, Polym. Adv. Technol. 28 (2017) 102–112.
504 <https://doi.org/10.1002/pat.3864>.

505 [54] G. Wacker, A.K. Bledzki, A. Chate, Effect of interphase on the transverse Young's
506 modulus of glass/epoxy composites, Compos. Part Appl. Sci. Manuf. 29 (1998) 619–
507 626. [https://doi.org/10.1016/S1359-835X\(97\)00116-4](https://doi.org/10.1016/S1359-835X(97)00116-4).

508 [55] L. Zhang, S. Lv, C. Sun, L. Wan, H. Tan, Y. Zhang, Effect of MAH-g-PLA on the
509 Properties of Wood Fiber/Poly(lactic acid) Composites, Polymers. 9 (2017) 591.
510 <https://doi.org/10.3390/polym9110591>.

511 [56] J. Borda, I. Bodnár, S. Kéki, L. Sipos, M. Zsuga, Optimum conditions for the
512 synthesis of linear poly(lactic acid)-based urethanes, J. Polym. Sci. Part Polym. Chem.
513 38 (2000) 2925–2933. [https://doi.org/10.1002/1099-0518\(20000815\)38:16<2925::AID-POLA100>3.0.CO;2-E](https://doi.org/10.1002/1099-0518(20000815)38:16<2925::AID-POLA100>3.0.CO;2-E).

515 [57] F. Zoukrami, N. Haddaoui, M. Sclavons, J. Devaux, C. Vanzeveren, Rheological
516 properties and thermal stability of compatibilized polypropylene/untreated silica
517 composites prepared by water injection extrusion process, Polym Bull. 75 (2018)
518 5551–5566. <https://doi.org/10.1007/s00289-018-2344-8>.

519 [58] X. Lin, K. Zhang, K. Li, D. Ren, Dependence of rheological behaviors of polymeric
520 composites on the morphological structure of carbonaceous nanoparticles, J. Appl.
521 Polym. Sci. 135 (2018) 46416. <https://doi.org/10.1002/app.46416>.

522 [59] D.H. Droste, A.T. Dibenedetto, The glass transition temperature of filled polymers
523 and its effect on their physical properties, J. Appl. Polym. Sci. 13 (1969) 2149–2168.
524 <https://doi.org/10.1002/app.1969.070131011>.

525 [60] A.N. Frone, S. Berlioz, J.-F. Chailan, D.M. Panaitescu, Morphology and thermal
526 properties of PLA–cellulose nanofibers composites, Carbohydr. Polym. 91 (2013)
527 377–384. <https://doi.org/10.1016/j.carbpol.2012.08.054>.

528 [61] H. Wang, X. Sun, P. Seib, Strengthening blends of poly(lactic acid) and starch with
529 methylenediphenyl diisocyanate, J. Appl. Polym. Sci. 82 (2001) 1761–1767.
530 <https://doi.org/10.1002/app.2018>.

531 [62] T. Ke, X. Sun, Physical Properties of Poly(Lactic Acid) and Starch Composites with
532 Various Blending Ratios, Cereal Chem. 77 (2000) 761–768.
533 <https://doi.org/10.1094/CCHEM.2000.77.6.761>.

534 [63] S.-Y. Lee, I.-A. Kang, G.-H. Doh, H.-G. Yoon, B.-D. Park, Q. Wu, Thermal and
535 Mechanical Properties of Wood Flour/Talc-filled Poly(lactic acid) Composites: Effect
536 of Filler Content and Coupling Treatment, J. Thermoplast. Compos. Mater. 21 (2008)
537 209–223. <https://doi.org/10.1177/0892705708089473>.

538 [64] M. Gaugler, W.J. Grigsby, Thermal Degradation of Condensed Tannins from Radiata
539 Pine Bark, 29 (2009) 305–321. <https://doi.org/10.1080/02773810903165671>.

540

One-step reactive extrusion

